RSC Advances

ROYAL SOCIETY OF CHEMISTRY

www.rsc.org/advances

Synergistic Toughening of Bioinspired Artificial Nacre by Polystyrene Grafted Graphene Oxide

Yanhong Wu, Rui Cao, LiangliangJi, Weichun Huang, Xiaoming Yang, and YingfengTu**

Suzhou Key Laboratory of Macromolecular Design and Precision Synthesis, Jiangsu Key Laboratory of Advanced Functional Polymer Design and Application, Department of Polymer Science and Engineering, College of Chemistry, Chemical Engineering and Materials Science, Soochow University, Suzhou 215123, P. R. China.

ABSTRACT: A biologically inspired, multilayer laminate structural design is deployed into composite films of polystyrene (PS) grafted graphene oxide (GO) synthesized by Ce(IV)/HNO_3 redox system in aqueous solution. Artificial hybrid films are fabricated using vacuum-assisted filtration macroscopic assembly method, using nacre as the structural model, GO as inorganic building blocks and PS as glue. The resulting multilayer structure and the mechanical property of the nanopaper were studied by scanning electron microscope, X-ray diffraction and stress-strain measurements. The resulting multilayer GO-PS films with low polymer content (<15 *vol* %) show greatly enhanced mechanical properties compared to pure GO films. And it is interesting

*Corresponding author. Tel.: +86 512 65884930. Fax: +86 512 65882130. E-mail address: yangxiaoming@suda.edu.cn (X.M. Yang). tuyingfeng@suda.edu.cn (Y.F.Tu).

that the mechanical properties of nacre-like films can be varied by the volume fraction of polymer.

1. Introduction

Nature possesses the capacity to construct biological materials (such as nacre, bone and wood) with extraordinary mechanical properties during lengthy natural evolution. Among these biomaterials, nacre is one of the most extensively studied materials. Nacre is composed of approximately 95 *vol* % aragonite calcium carbonate ($CaCO_3$) platelets and 5 *vol* % biomacromolecules. The computational study demonstrated that thin layers of polymer are capable of hindering cracks from propagating, yielding a defect-tolerant composite with increased overall strength.[1] In other words, natural nacre has a nano/microscale hierarchical structure and precise inorganic-organic interface, which enables it to achieve a unique combination of light weight, remarkable strength, and toughness. From a mechanical point of view, nacre is often simplified as a binary composite, where hard, two-dimensional (2D) aragonite platelets and soft biopolymer layers are alternately stacked into a "brick-and-mortar" structure. Thus far, intense efforts have been devoted to mimicking the "brick-and-mortar" microstructure of nacre by assembling different types of 2D inorganic platelets and polymer matrices. 2D micro/nanoparticles, such as layered double hydroxide,[2] clay[3] and alumina

platelets,[4] have been widely used as the "bricks". However, exploring new rigid platelet-like inorganic particle as building block for construction of nacre-like structures is essential.

Graphene is regarded as a good candidate of building block for fabricating biomimetic composites in recent years, owing to its 2D sheet morphology, extraordinary mechanical properties and high conductivity.[5] Graphene can also broaden the potential applications of nacre-like artificial materials, because it can endow the biomimetic materials with additional functionality such as flexibility and conductivity. However, discussion in the literature of multi-functional design of artificial nacre has been very limited.[6]

Here we introduce a "bottom up" strategy to prepare biomimetic materials by polymer-grafted graphene oxide as building blocks, where the local phase separation is fundamentally avoided and strong interfacial interaction is introduced simultaneously. 2D GO is selected as the ideal "brick", and a well-studied polymer, polystyrene, as "mortar" to construct the layered architecture. Polystyrene (PS) grafted graphene oxide (GO) was synthesized by Ce(IV)/HNO_3 redox system in aqueous solution. Redox reaction systems of Ce (IV) salts with reducing agents in aqueous solution are well known initiators for vinyl polymerization.[7-10] Since there are a lot of hydroxyl groups on GO surface, these groups can be used as reducing agents to initiate polymerization of styrene monomers if coupled with Ce (IV) salts. In our previous work, vinyl polymer chains were covalently bonded onto the nanosheets through redox system, using cerium (IV) ammonium nitrate/nitric acid and GO's hydroxyl group as the redox couple.[11] As the

hydroxyl functional groups are attached above and below each carbon layer, the grafted PS brushes are distributed on the surface of GO, rather than around the edge of GO. Compared to other methods, the redox reaction systems have the prime advantage of operating in aqueous solution at a very moderate temperature, and the polymer grafted GOs are easily to be obtained by filtration or centrifugation, thus is more green compared to those reaction carried out in organic solvents. According to our previous report, the volume fraction of polymer can be controlled below 15%, resulting in the perfect layered structure. In this study, PS functionalized GO sheets were used as building block to form artificial nacre since perfect layered structure retained. Vacuum-assisted filtration macroscopic assembly method was used to prepared artificial nacre.[12] Compared with other assembly techniques,[13] such as layer-by-layer deposition,[14] ice-template assembly,[15] electrophoretic deposition[16] and evaporation-induced self-assembly,[17] the vacuum-assisted filtration assembly technique is an economical, simple, fast and large-scale fabrication method of preparing bio-inspired layered materials. Several mechanisms have been suggested for the self-alignment of 2D GO and GO-PS in the process of vacuum-assisted filtration and macroscopic assembly, such as gravitational force, shear flow and the excluded volume effect.[18] During thevacuum-assisted filtration process, with the increasing concentration of GO or GO-PS, the interparticle distance decreased. GO or GO-PS at high concentrations tends to self-assemble into a layered structure.[18-20] In this paper, for the novel artificial nacre films, the influence of mechanical properties properties such as Young's modulus, tensile strength and toughness by changing PS content was studied.

2. Experimental

2.1 Materials

Graphite was purchased from Uni-Chem. N,N-dimethylformamide (DMF), sodium hydroxide,styrene (St)，alcohol and nitric acid (65-68*wt*%) were purchased from Sinopharm Chemical Reagent Co., Ltd. St was washed by 5*wt*% sodium hydroxide aqueous solution and vacuum-distilled to remove the inhibitor prior to polymerization. Ceric ammonium nitrate (CAN) (Aldrich) was used without further purification. Stock solutions of Ce(IV) were prepared from CAN in aqueous nitric acid (1 mol/L).

2.2 Synthesis of PS grafted GO

The well-dispersed GO was synthesized from natural graphite using a modified Hummers method,[21-23] and stored in stock aqueous suspensions at a certain concentration. The synthesis of PS grafted GO is similar to our previous report.[11] A typical operation procedure of synthesis of PS grafted GO is given as follow: 50 mg GO was dispersed in 90 mL deionized water, then transferred into a 4 neck round bottom flask and sonicated in sonic bath for 30 min followed by introducing 2 mL St monomer. The solutions were purged with nitrogen for the duration of preparation. Appropriate amount (0.05g, 0.10 g, 0.15g) of CAN in 1 mol/L nitric acid solution was then added to the reaction mixture by drops for about 5 min while stirring under nitrogen atmosphere. The polymerization experiments were conducted with stirring at 80 °C for 24 hours.

2.3 Preparation of GO-PS film

After polymerization, the products were collected by vacuum filtration, washed by alcohol until no white drops in the water was found. The product was redispersed in DMF. The GO or GO-PS dispersion was then vacuum filtered through a Millipore filter (47mm in diameter and 0.45 μm in pore size). Subsequently, the filters supported GO or GO-PS film was dried under vacuum, and then peeled off under the circumstance of alcohol. The thickness of the as-prepared free-standing GO or GO-PS film was about 30 μm.

2.4 Characterization

Thermal gravimetric analysis (TGA) was carried out using Perkin-Elmer Pyris 6 TGA instrument with a heating rate of 10 °C/min under a nitrogen flow. XPS measurements were performed using an ESCALAB 250 instrument (Thermo Electron) with Al KR radiation. The fracture surface images were obtained using scanning electron microscope (SEM, Quanta FEG250). Mechanical properties were tested by Instron-3365 with gauge length of 10 mm, and loading rate of 0.5 mm/min. All the samples were cut into strips with the length of 30 mm and the width of 3 mm. The sample thickness was obtained from SEM imaging of the fracture edge. The results for each material are based on 10 specimens. X-ray diffraction (XRD) analysis was performed on X'Pert-Pro MPD diffractometer with a Cu K radiation source at room temperature. Raman spectra were recorded from 800 to 3600 cm^{-1} with a Renishaw spectrometer using a 514 nm argon ion laser.

3. Results and discussion

In this study, three samples with different volume fraction of PS were prepared by varying the concentration of initiator. The formation mechanism by simple and easy vacuum-assisted filtration assembly technique of the hybrid film is schematically presented in Figure 1. According to the previous study, PS chains covalently were bonded to GO via oxygen.[11] As the GO itself possess quite strong hydrogen bonding interaction, the hydrogen bonding interaction still exist in GO/PS system. At the same time, PS chains with randomly coiled conformation may form entanglement network but there are no bonding between PS chains.

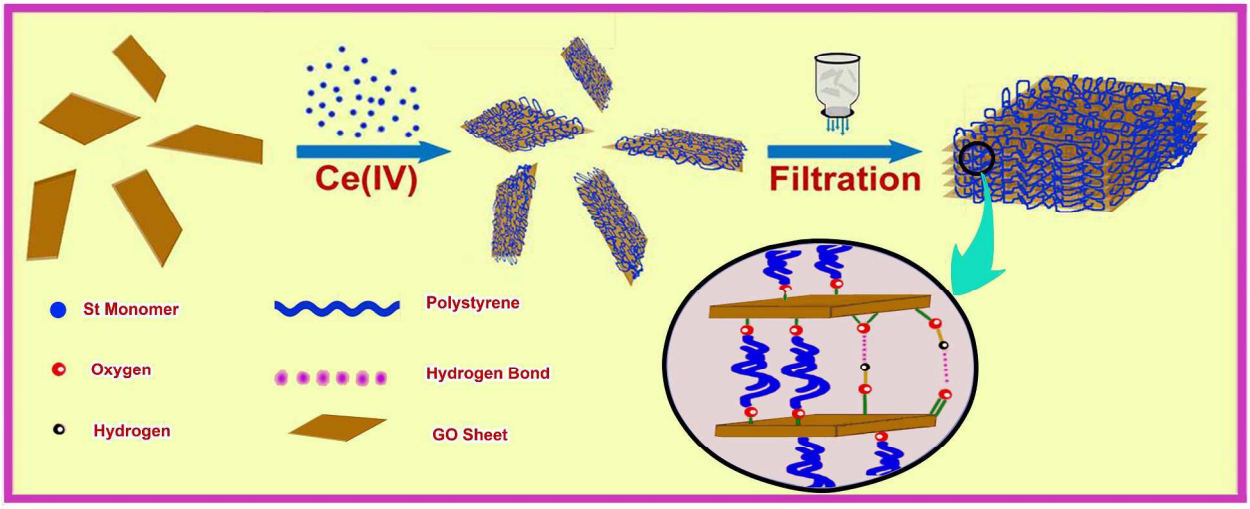

Figure 1. Synthesis of GO-PS building blocks and vacuum filtration assisted assembly approach to hybrid film.

The obtained films by vacuum filtration assisted assembly approach were showed as Figure 2. Figure 2a & 2b revealed that brown, semi-transparent and free-standing GO film with the

thickness in the range of 30 μm was successfully prepared. The thickness of the membrane can be tuned by the amount of the sample. The color of GO-PS paper turns black, as was showed in Figure 2c & 2d the possible reason is that GO was partly thermal reduced in the process of polymerization, which can be proved by XPS and Raman results, which will be discussed below. Figure 2b & 2d also indicates that both films are flexible. The surfaces of both films are very smooth suggesting the macroscopic uniformity of films.[6]

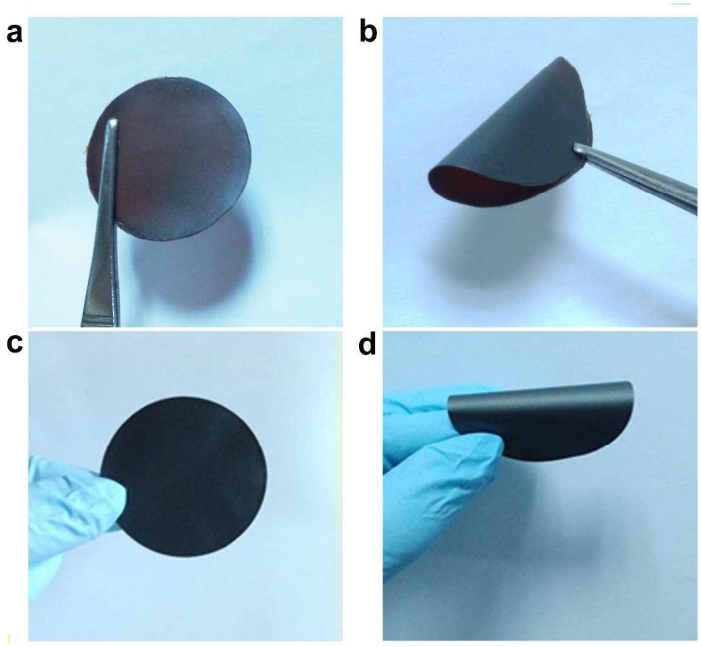

Figure2. Digital photos of (a, b): GO; (c, d): hybrid film demonstrating its flexibility.

It is important to determine the content of PS in hybrid film. The volume fractions of PS were estimated by TGA technique. TGA measurements are used to estimate the percentages of PS and can investigate the thermal stability of materials. As shown in Figure 3, the weight loss of

GO started below 100 °C during the heating process, which was due to the evaporation of absorbed water. From 100 to 250 °C, the weight loss of GO should be attributed to both the evaporation of absorbed water and the pyrolysis of the oxygen-containing functional groups. When the temperature is above 250 °C, the weight loss of GO should arise from the release of oxygen away from GO. At the temperature of 460 °C, the residual weight of GO is around 45%, indicating that the degraded part of GO is around 55%. By comparison with the curve of GO, it can be concluded that the first weight loss stages of GO-PS below 100 °C and the second one at around 210 °C are coming from the decomposition of GO, corresponding to the pyrolysis of physically and chemically bonded water molecules and hydroxyl groups respectively. The third stage, which is about 400 °C is mainly corresponding to the decomposition of grafted polymer. The same phenomena were observed from PS grafted GO composite synthesized by other method.[23]

The weight fraction of PS in the resulting hybrid films was determined by the weight loss between 232 and 460 °C. The weight loss of GO in this range was deducted. The weight fraction of PS in the composite films is 9.8, 2.7and 2.0 *wt*% determined by TGA. The volume fraction of PS is calculated by using the weight fraction and density of GO (1.3 g/cm^3) and PS (1.04 g/cm^3), respectively.[11, 24]

$$V_2\% = \frac{\frac{w_2}{\rho_2}}{\frac{w_1}{\rho_1} + \frac{w_2}{\rho_2}}\% \qquad (1)$$

Where, V_2 %: the volume fraction of PS; w_1 %: the weight fraction of GO; w_2 %: the weight fraction of PS.

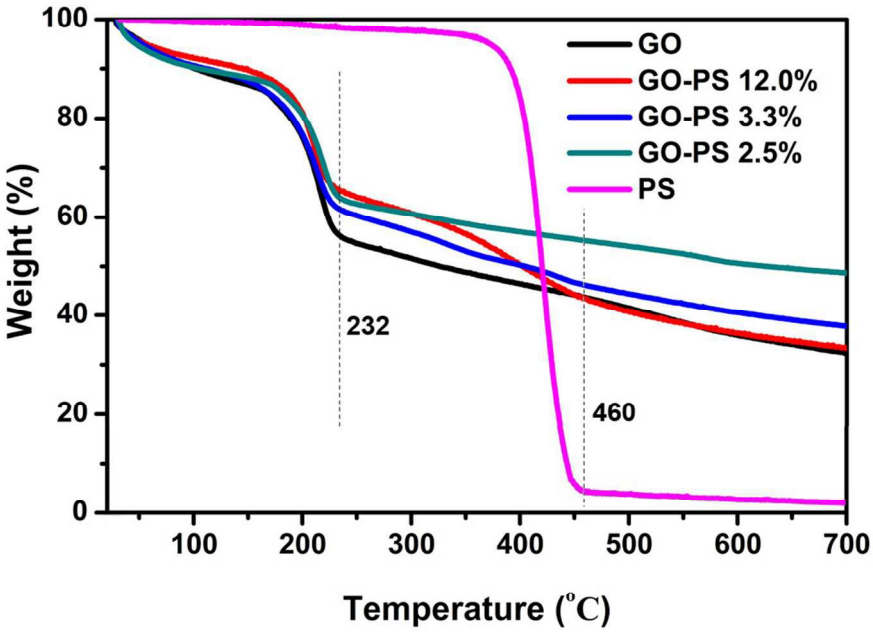

Figure 3. The TGA curves of pure GO, GO-PS 12%, GO-PS 3.3% and GO-PS 2.5%.

The volume fraction of PS in the composite films is 12, 3.3 and 2.5*vol*% determined by equation (1). Hereafter, the hybrid films would be denoted as GO-PS x%, where the x is the volume content of PS in the composite film. For GO-PS, the weight loss proportion below 250 °C is still quite high, indicating that there are high portions of oxygen-containing groups on the surface of GO after polymerization. This is due to the fact that there are many epoxides groups on the surface of GO and they cannot work with reducing agent in our polymerization

process. However, these oxygen-containing groups are very important for the interface interaction of hybrid film.

The surface atomic composition of GO and GO-PS was investigated by XPS. Figure 4 displays the XPS survey spectra of GO and GO-PS and the corresponding XPS data are summarized in Table 1. The broad C1s peak of the pure GO，GO-PS can be fitted into four peaks with the binding energy at 284.7, 285.7, 287.7, and 289.1 eV, corresponding to the C-C, C-O, C=O, and C(O)O groups, respectively.[25] Carbon to oxygen (C/O) ratio obtained from XPS analysis is one of the most widely employed evaluation criteria for quantifying reduction degree of reduced GO. Accordingly, the ratio of C1s to O1s is increased significantly after grafted PS (shown in Table 1). C/O ratio of GO is 0.843, while those of GO-PS are 1.95 (12%), 2.15 (3.3%) and 1.13 (2.5%), respectively, indicating deoxygenation in the process of graft polymerization reaction.

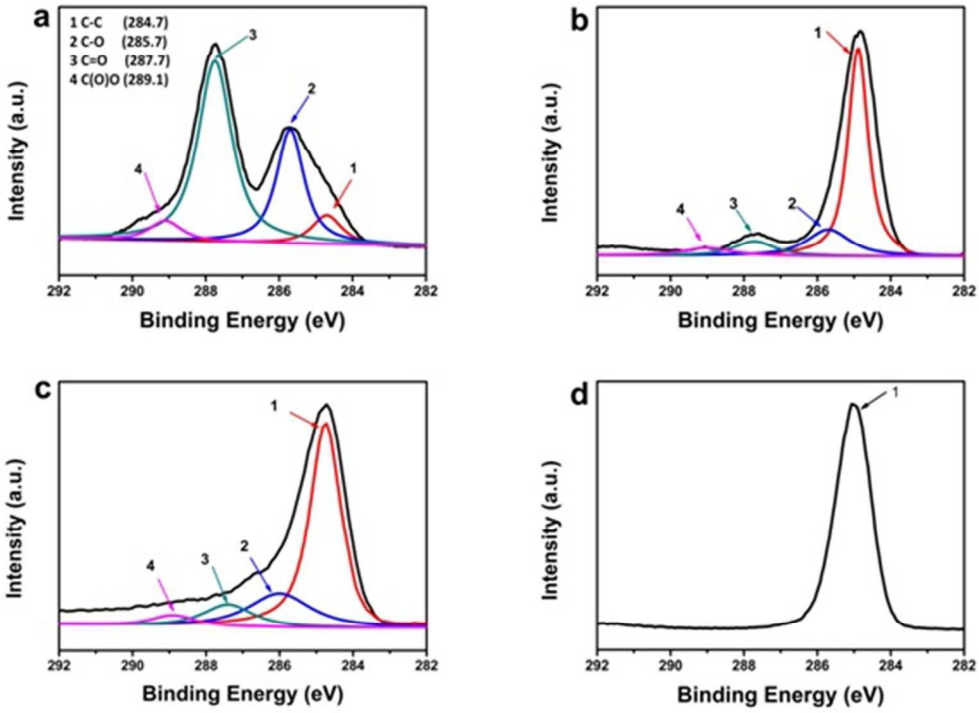

Figure 4. XPS of (a): sample pure GO, (b): GO-PS 12%, (c): GO-PS 3.3%, (d): GO-PS 2.5% films.

Table 1. Values of C/O atomic ratios obtained by the XPS analysis.

Sample	GO	GO-PS 12%	GO-PS 3.3%	GO-PS 2.5%
C/O Ratios	0.843	1.95	2.15	1.13

Raman spectroscopy is a powerful tool for investigating the structure of carbonaceous materials. The Raman spectra of GO and GO-PS show two distinct peaks at 1347 and 1605 cm^{-1} (Figure 5). The intensity ratio of D and G bands expresses the sp^3/sp^2 carbon ratio, a measure of the extent of disorder (shown in Table 2), but it does not always reflect the oxidation or reduction

degree, because the ID/IG ratio can be influenced by edges, charge puddles, ripples, or many other defects.[26] For instance, Ruoff et al. has reported that reduced GO has an increased I_D/I_G ratio than GO.[27] While Shi et al. reported that reduced GO has a decreased I_D/I_G ratio than GO.[28] The I_D/I_G ratio has no obvious variation compared to initial GO. The value of I_D/I_G for GO-PS increases a little bit and blue shifts of D and G bands are observed in the Raman spectrum, suggesting decrease of oxygen-containing groups and interaction between GO and PS.[29]

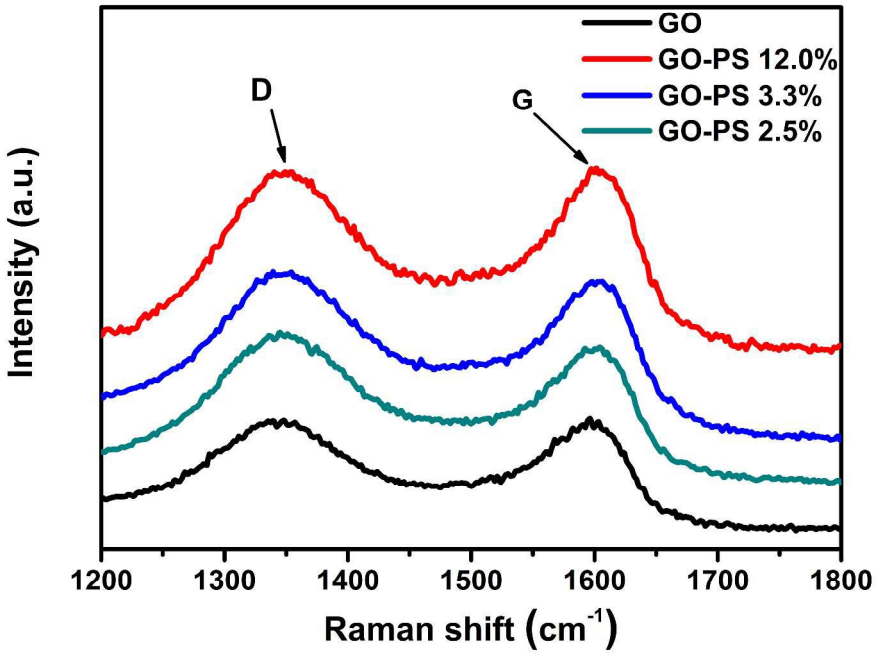

Figure 5. Raman spectra of pure GO, GO-PS 12%, GO-PS 3.3%, GO-PS 2.5%.

Table 2. The comparison of peak intensity D band and G band

Sample	Pure GO	GO-PS 12.0%	GO-PS 3.3%	GO-PS 2.5%

I_D/I_G	0.98	1.01	1.09	1.12

To further investigate the layered structure of GO-PS film, XRD patterns of GO and GO-PS films were recorded. In Figure 6, the XRD peak of the pristine was observed at 2θ=10.8°, indicating the interlayer distance of 8.135 Å. After PS incorporated onto GO, the peak shift to 8.79° for GO-PS 12% with corresponding layer thickness of 10.055 Å, and to 10.65° for GO-PS 3.3% with a corresponding layer distance of 8.302 Å, and further to 10.55° for GO-PS 2.5% with a corresponding layer distance of 8.381 Å. These peaks indicate that the ordered layer structure remains after polymerization, with the PS intercalated between GO layers to form an intercalated structure (shown in Figure 1). In addition, the peak shift to lower angle indicates an increase of the layer thickness with increasing the content of PS, which is consistent with the results of TGA. The above results confirm that our hybrid film has a nacre-like structure, in which 2D GO sheets is stacked and glued together effectively by PS. The hybrid layered structure model of resultant artificial nacre is proposed as shown in Figure 1.

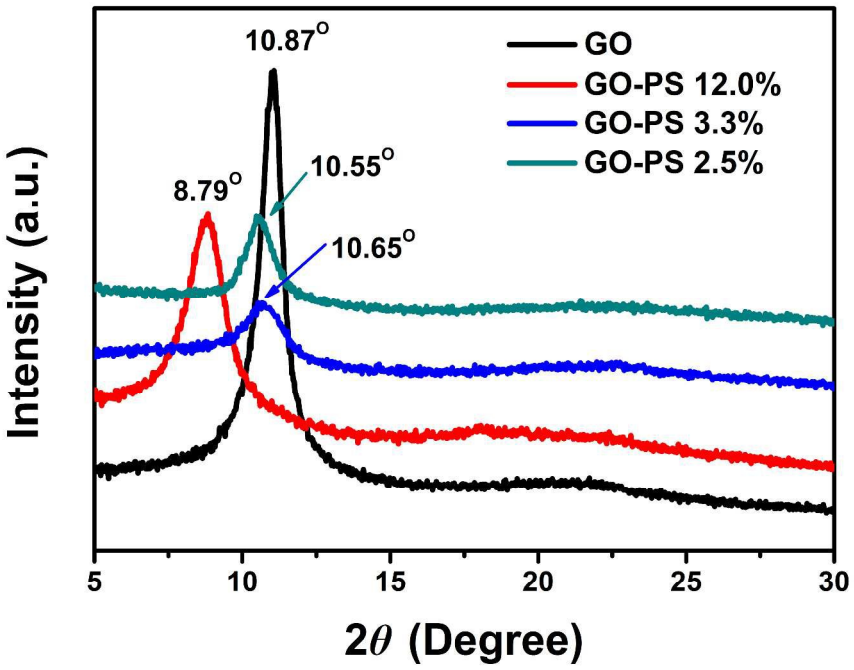

Figure 6.XRD curves of GO and GO-PS.

The artificial nacre-like materials shows interesting property of high mechanical performance, due to their special "brick-and-mortar" structures. The typical tensile stress-strain curves of the nacre-inspired composite are shown in Figure 7. The tensile stress at break, strain at break, Young's modulus, and toughness are summarized in Table 3. The stress-strain curves of all samples exhibit three regions, namely initial straightening (I), elastic (II) and plastic (III) regions,

similar to those described in GO papers, which were separated by dashed lines in Figure 7.[30]

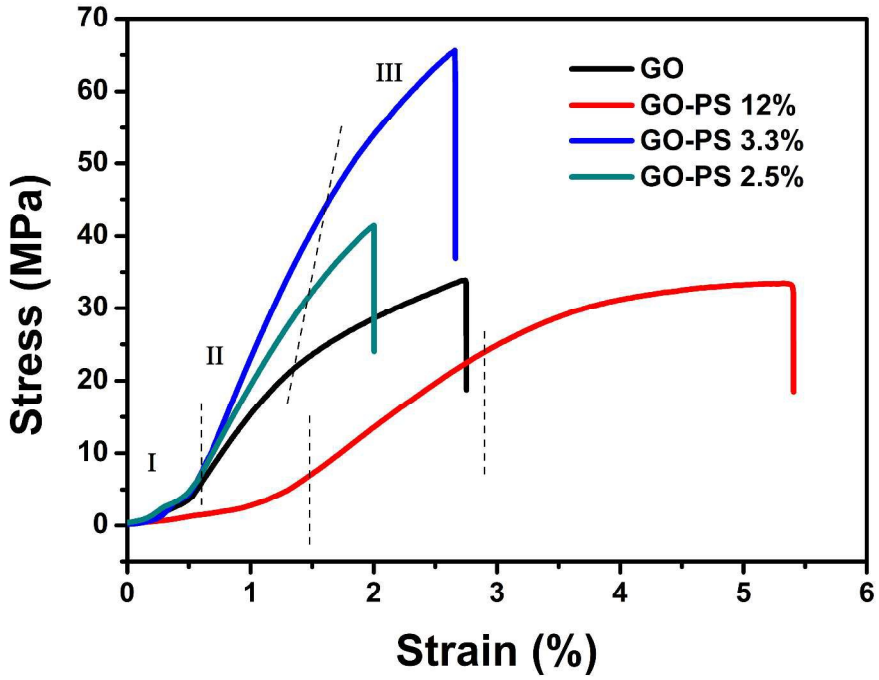

a: dashed lines separate curves into three segments Ⅰ, Ⅱ, Ⅲ

Figure 7. Tensile stress-strain curves for GO and artificial nacre films with different PS content.[a]

Table 3. Mechanical Properties of nacre-like films with different of PS content[a]

Samples	Tensile strength (MPa)	Ultimate strain (%)	Young's modulus (GPa)	Toughness ($MJ \cdot m^{-3}$)

GO	34.3	2.61	2.43	0.51
GO-PS 12%	36.9	5.54	1.46	1.15
GO-PS 3.3%	66.5	2.99	3.75	0.95
GO-PS 2.5%	34.2	2.02	2.55	0.34

a: Values are averaged from ten artificial nacre samples

The volume fraction of PS directly affects mechanical properties of the composite films. The tensile strength and Young's modulus of artificial nacre films increase from 34.3 MPa and 2.43 GPa for pure GO to 66.5 MPa and 3.75 GPa at V=3.3 *vol*%, (V means the volume content of PS) respectively. At the same time, the strain at break is maintained. The results are consistent with the reported values for other artificial nacre films based on GO.[31, 32] However, when the volume content of PS increases to *V*=12 *vol*%, the tensile strength is maintained. While the strain increase to 5.54%, while the Young's modulus decrease from 24.3 to 14.6 GPa. The toughness calculated from the areas under the sress-strain curves reaches the 1.15 MJ•m^{-3} at *V*=12 *vol*%, comparable to that of natural nacre (1.8 MJ•m^{-3}).[31] For artificial nacre film with low PS content (*V*=2.5 *vol* %), the mechanical properties (the tensile strength, strain to failure, Young's modulus, and toughness) is the same as that of GO without PS. The possible reason is that the PS content is too low to affect the final properties of the materials.

In conclusion, GO-PS films show a unique tensile behavior. The mechanical properties of nacre-like films can be varied by the volume fraction of polymer. After linear elastic deformation, a plastic deformation appears. The initial elastic modulus, stress at break, and the toughness significantly increased with increasing the content of PS. The Young's modulus, stress at break and toughness for the artificial nacre films at V= 3.3 *vol*% were improved by 54, 94 and 88%, respectively. For the sample with PS content increased to 12 *vol*%, the onset of the plastic deformation occurs at a high strain from 0.5 to 1.0% (Figure 7). Furthermore, the toughness and the strain to failure were improved by 127 and 112%, respectively. However, the Young's modulus decreased by 66% and the tensile strength was maintained.

The excellent mechanical properties are attributed to the layered nanoscale structure and unique GO/PS interfacial interaction, that is the synergistic interaction between GO and PS Great synergistic interactions between GO and nanofibrillated cellulose were clearly identified, which led to a noticeable improvement in the mechanical properties of hybrid fibers compared with fibers made solely from one of the two building blocks. [33] In the layered structure, PS chains are uniformly dispersed between two GO sheets. Hence, in the homogeneous GO/PS layered structure, the load of GO sheets is spread over many PS chains. However, as the GO itself possess quite strong hydrogen bonding interaction, the hydrogen bonding interaction still exist in GO/PS system. Moreover, PS chains with randomly coiled conformation may form entanglement network and act as glue. When loading, the PS chains and GO sheets extensively slide against

each other. As a result, the process with large deformation is accompanied by dissipation of a large amount of energy. Larger amount of PS results in large amount of energy dissipation and high toughness.

Unfortunately, the mechanical performance of these films is inferior to some nacre-mimicking materials, [34] which may be due to high oxidation degree of GO compared with other reported GO. Although the mechanical performance of our hybrid films is not superior to that reported in the literature, the synergistic effect of improving the mechanical properties of the films is clearly demonstrated. The high oxidation degree of GO may destroy conjugated structure of GO sheets, which will cause poor mechanical property. The weak interfacial interaction between PS chains in these films should be another reason. Other polymers with strong interfacial interaction such as hydrogen bond interaction or crosslinked interaction will be studied in the future work.

To clarify the structure change in the tensile process, we observed the characteristic fracture morphology of artificial nacre films by SEM. Figure 8 demonstrates the fracture morphology of pure GO and the artificial nacre, displaying that PS are indeed present and dispersed between GO sheets. The SEM images also reveal that the 2D nanosheets of GO and GO-PS are densely assembled into layered nanostructure, which is comparable to natural nacre. Pulling out of the GO and GO-PS sheets can be clearly discerned. The fracture mechanism is obviously different with other reported GO or reduced GO reinforced polymer composites, but identical to the

natural nacre.[35] The SEM of the cross-section of GO-PS 2.5% (Figure 6 (d)) confirmed the highest content of PS.

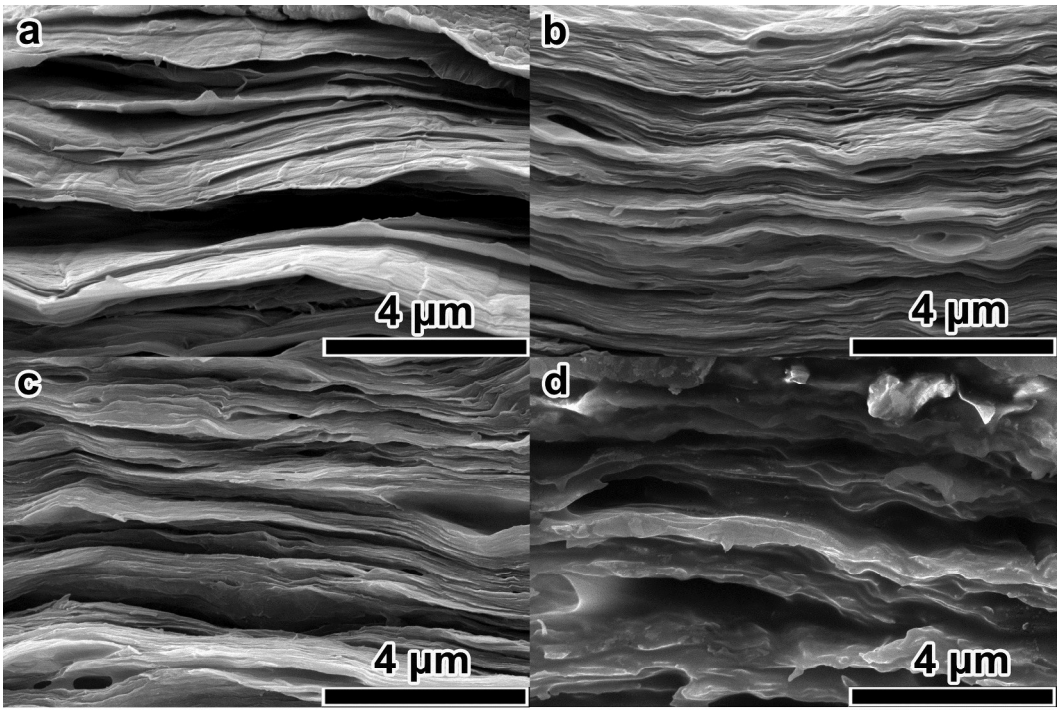

Figure 8. SEM images of the cross-section of artificial nacre based on GO, showing a highly aligned layered arrangement. (a): GO; (b): GO-PS 12%; (c): GO-PS 3.3%; (d): GO-PS 2.5%.

4. Conclusions

We have successfully fabricated lightweight, free-standing artificial nacre film by simple vacuum-filtration self-assembly using cerium (IV) ammonium nitrate/nitric acid and GO's hydroxyl group as the redox couple. The layered composite possesses artificial nacre like brick-and-mortar arrangement of organic (PS) and inorganic (GO) layers and shows strong mechanical

properties. These results provide a new concept for the design and preparation of high-performance materials combination of high strength, toughness and high conductivity for potential applications, such as sensors, artificial muscles and environmentally friendly materials.

Acknowledgment

The financial support from the National Natural Science Foundation of China (No. 21104050), China Postdoctoral Science Foundation (2013M541715, 2014T70541), a Project Funded by the Priority Academic Program Development of Jiangsu Higher Education Institutions are gratefully acknowledged.

References

1 A. M. Beese, Z. An, S. Sarkar, S. S. P. Nathamgari, H. D. Espinosa and S. T. Nguyen, A*dv. Funct. Mater.*, 2014, **24**, 2883-2891.

2 M. Q. Zhao, Q. Zhang, J. Q. Huang and F. Wei, *Adv. Funct. Mater.*, 2012, **22**, 675-694.

3 A. Walther, I. Bjurhager, J. M. Malho, J. Ruokolainen, L. Berglund and O. Olli Ikkala, *Angew. Chem. Int. Ed.*, 2010, **49**, 6448-6453.

4 E. Munch, M. E. Launey, D. H. Alsem, E. Saiz, A. P. Tomsia and R. O. Ritchie, *Science*, 2008, **322**, 1516-1520.

5 X. Zhao, Z. Xu, B. Zheng and C. Gao, *Sci. Rep.*, 2013, **3**, 3164.

6 D. Zhong, Q. L. Yang, L. Guo, S. X. Dou, K. S Liu. and L. Jiang, *Nanoscale*, 2013, **5**, 5758-5764.

7 C. Erbil, A. B. Soydan, A. Z. Aroguz and A. S. Sarac, *Die. Angew. Makromol. Chem.*, 1993, **213**, 55-63.

8 C. Erbil, A. B. Soydan, A. Z. Aroguz and A. S. Sarac, *J. Appl. Polym. Sci.*, 1993, **47**, 1643-1648.

9 B. Dincer, S. Bayulken and A. S. Sarac, *J. Appl. Polym. Sci.*, 1997, **63**, 1643-1647.

10 C. Ozeroglu, O. Guney, A. S. Sarac and M. I. Mustafaev, *J. Appl. Polym. Sci.*, 1996, **60**, 759-765.

11 L. J. Ma, X. M. Yang, L. F. Gao, M. Lu, C. X. Guo, Y. W. Li, Y. F. Tu and X. L. Zhu, *Carbon*, 2013, **53**, 269-276.

12 K. W. Putz, O. C. Compton, C. Segar, Z. An, S. T. Nguyen and L. C. Brinson. *ACS. Nano.*, 2011, **5**, 6601-6609.

13 J. Wang, Q. Cheng, L. Lin and L. Jiang, *ACS. Nano.*, 2014, **8**, 2739-2745.

14 A. Y. Sham and S. M. Notley, *Langmuir*, 2014, **30**, 2410-2418.

15 S. Deville, E. Saiz, R. K. Nalla and A. P. Tomsia, *Science,* 2006, **311**, 515-518.

16 C. A. Wang, B. Long, W. Lin, Y. Huang and J. Sun, *J. Mater. Res.,* 2008, **23**, 1706-1712.

17 B. Yuan, C. Bao, X. Qian, L. Song, Q. Tai, K. M. Liew and Y. Hu, *Carbon*, 2014, **75**, 178-189.

18 N. Yousefi, M. M. Gudarzi, Q. B. Zheng, S. H. Aboutalebi, F. Sharif and J. K. Kim, *J. Mater. Chem.*, 2012, **22**, 12709-12717.

19 N. Yousefi, X. Lin, Q. B. Zheng, X. Shen, J. R. Pothnis, J. J. Jia, E. Zussman and J. K. Kim, *Carbon*, 2013, **59**, 406-417.

20 B. Dan, N. Behabtu, A. Martinez, J. S. Evans, D. V. Kosynkin, J. M. Tour, M. Pasquali and II. Smalyukh, *Soft.*, *Matter.* 2011, **7**, 11154-11159.

21 W. S. Hummers and R. E. Offeman, *J. Am. Chem. Soc.*, 1958, **80**, 1339-1339.

22 V. C. Tung, M. J. Allen, Y. Yang and R. Kaner, *Nat. Nanotechnol.*, 2009, **4**, 25-29.

23 X. M. Yang, L. J. Ma, S. Wang, Y. W. Li, Y. F. Tu and X. L. Zhu, *Polymer*, 2011, **52**, 3046-3052.

24 J. Brandrup, E. H. Immergut and E. A. Grulke, Polymer Handbook (Fourth Edition), A Wiley -Interscience Publication, USA 1999.

25 D. Luo, G. Zhang, J. Liu and X. Sun, *J. Phys. Chem. C*, 2011, **115**, 11327-11335.

26 C. N. R. Rao, A. K. Sood, K. S. Subrahmanyam and A. Govindaraj, *Angew. Chem. Int. Ed*, 2009, **48**, 7752-7777.

27 S. Stankovich, D. A. Dikin, R. D. Piner, K. A. Kohlhaas, A. Kleinhammes, Y. Jia, Y. Wu, S. T. Nguyen and R. S. Ruoff, *Carbon,* 2007, **45**, 1558-1565.

28 Y. Wang, J. R. Yu, L. Chen, Z. M. Hu, Z. X. Shi and Z. Zhu, *RSC. Adv.*, 2013, **3**, 20353-20362.

29 S. Huang, H. D. Peng, W. W. Tjiu, Z. Yang, H. Zhu, T. Tang and T. X. Liu, *J. Phys. Chem. B*, 2010, **114**, 16766-16772.

30 D. A. Dikin, S. Stankovich, E. J. Zimney, R. D. Piner, G. H. Dommett, G. Evmenenko, S. T. Nguyen and R. S. Ruoff, *Nature,* 2007, **448**, 457-460.

31 Q. F. Cheng, M. X. Wu, M. Z. Li, L. Jiang and Z. Y. Tang, *Angew. Chem. Int. Ed,* 2013, **52**, 3750-3755.

32 O. C. Compton, S. W. Cranford, K. W. Putz, Z. An, L. C. Brinson, M. J. Buehler and S. T. Nguyen, *ACS. Nano.*, 2012, **6**, 2008-2019.

33 Y. Li, H. Zhu, S. Zhu, J. Wan, Z. Liu, O. Vaaland, S. Lacey, Z. Fang, H. Dai, Teng Li and L. Hu, *NPG Asia Materials*, 2015, **7**, 1-10

34 J. F. Wang, Q. F. Cheng and Z. Y. Tang, *Chem. Soc. Rev.*, 2012, **41**, 1111-1129.

35 L. J. Bonderer, A. R. Studart and L. J. Gauckler, *Science,* 2008, **319**, 1069-1073.